Dependence of the statistics of optical flares due to specular reflections from sea surface on the local surface slopes

A.S. Zapevalov

Naval Geophysical Institute of National Academy of Sciences, Sevastopol, Ukraine

Received September 13, 2000

We analyze the *in situ* measurements of local sea surface slopes, as well as the data of simultaneous laser sensing along nadir. The measurements were conducted from an oceanographic platform in the Black Sea, off the coast of the southern Crimea. It is shown that the relation of integral parameters of a series of flares due to specular reflections from sea surface and local sea surface slopes has statistical nature. Correlation matrices and regression equations are calculated to describe this statistics.

Introduction

Fine topographic structure of sea surface, formed by short wind waves, is very sensitive to such factors as wind velocity, internal waves, currents, atmospheric boundary layer (BL) stratification, upwelling, concentration of surface-active species, etc. By measuring the variations of the surface fine structure, conducive to scattering of electromagnetic fields, it is in principle possible to monitor remotely the processes in the boundary layers of the atmosphere and ocean.[1,2]

Despite its importance, the response of the sea surface to variations in the BL parameters is yet poorly understood. This, on the one hand, is due to technical problems arising in the measurements of short-period wind waves in sea; and, on the other hand, because the theoretical analysis is very complicated as it necessarily, deals with many nonlinear interactions between physically diverse factors. Therefore, to refine and update the remote sensing methods and techniques, we performed a series of field experiments under well controlled conditions, which allowed us to compare the data of the radar-type observations with the data of *in situ* measurements of the sea surface slopes (see, e.g., Refs. 3 and 4). To our knowledge, this was the first complex study of that kind in which laser sensing data were compared with the measurement data on the sea surface slopes.

Normally, the scattering by the sea–atmosphere interface is modeled by use of moving random Gaussian surface. This model was first employed in Ref. 5, and then it found several applications more. At the same time, the field studies indicate that the two-dimensional probability distribution of the along- and cross-wind components of the sea surface slopes is not strictly normal.[6–8] The distribution of along-wind slope component is asymmetrical, and its skewness varies with the varying wind speed. The experimental value of kurtosis is somewhat higher than that for normal distribution. In addition, the shape of the distribution of modulus (or total) slope depends essentially on the azimuth distribution of the wave components energy,[5] whose behavior in the high-frequency region has not yet been well studied.

All this makes it necessary a direct comparison of sensing data in the optical wavelength range with *in situ* measurements of the parameters that determine the sea surface roughness. The goal of this study is to investigate the statistics of specular reflections in nadir laser sensing and its relation to the characteristics of sea surface slopes.

Instrumentation and measurement conditions

We used two types of instruments: a "Feniks" laser sensor and a "Ryab" two-dimensional meter of sea surface slopes. The Feniks sensor used was designed and manufactured at the Leningrad Institute of Airborne Instrumentation Making according to technical specifications from Naval Hydrophysical Institute. The sensor includes coaxial receiver and transmitter of optical signals (Fig. 1*a*). In the figure, signal from the transmitter *1* (a He–Ne laser) of LGI–203 type with the power of 4 mW, is directed by the prism *3* through the objective *4* to the water surface. The specularly reflected beam, falling within the objective, is redirected, again by prism *4*, toward the photodetector *2*.

In the case of normal incidence, undisturbed water surface reflects about 2% of incident energy, while the disturbed one reflects somewhat less amount of energy. To record specularly reflected signal under conditions of strong wind and considerable surface disturbance, we used the photodetector with the threshold sensitivity at the level of 0.06% of the laser beam energy incident upon the sea surface.

Laser sensing was performed along nadir from 5-m height, so that the spot diameter at the undisturbed surface was 5 mm. When oriented along nadir, the photodetector records only sun glares formed by the surface fragments whose local slopes are less than some threshold ξ_{th}. From simple geometrical considerations[9] it follows that the ξ_{th} value is determined by the

0235-6880/00/12 1039-04 $02.00

diameter d of the receiver aperture and the distance h from the receiver to the reflecting surface: $\xi_{th} = d/(4h)$. In our experiment, $d = 5$ cm and $h = 500$ cm; hence $\xi_{th} = 0.0025$. We note that the distance to the sea surface is not fixed and varies due to the presence of long wind waves and ripples. For the measurement series analyzed here, the rms wave amplitude was less than 15 cm, and the corresponding ξ_{th} variations did no exceed ±3%.

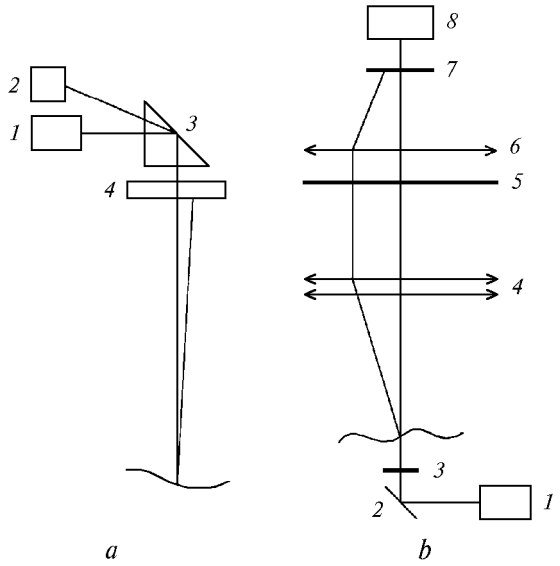

Fig. 1. Block-diagrams of Feniks (*a*) and Ryab (*b*) sensors.

For measurements of the sea surface slopes, we used a "Ryab" two-dimensional (2D) sea surface inclinometer designed jointly by the Naval Hydrophysical Institute and the Polytechnic Institute in Kiev. The optical layout of the laser inclinometer is depicted in Fig. 1*b*. An LGN–208A laser *1*, installed in a hermetically sealed container, was used as a light source. The laser beam is reflected from the mirror *2*, passes through the protective glass *3*, crosses the sea surface, and then it is collected by an objective with the focal length of 600 mm, assembled from two identical lenses *4*. Then the beam is projected onto an mat screen *5* and collected by the lens *6*. We used a TV camera as the image converter in which a CCD array *8* is used as a sensitive element. The TV camera is equipped with an interference filter *7* centered at the wavelength 0.63 μm.

The laser inclinometer is described in Ref. 10; essentially, it measures angular deviations of the laser beam as it passes (from under the sea surface) through rough sea–air interface. The recorded angle of deviation of the laser beam from vertical is determined by local slope of sea surface at the point where laser beam intersects the surface (on surface fragment ~ 2 mm^2 area).

The sensor has the following specifications: the range of measured slopes ±30°; measurement error (as determined in laboratory tests) is 0.2°; permissible height of sea waves is up to 1 m; and sampling rate is 0.02 s.

The measurement points of specular reflection characteristics of laser beam and those of local sea surface slopes were spatially separated by no more than 4 m. The "Ryab" inclinometer and "Feniks" optical sensor measurements were synchronized relative to starting time and duration, both between themselves and with the meteorological measurements (wind speed and direction and air temperature). The duration of a single measurement cycle was 30 s.

The sea surface structure was studied using oceanographic platform of the Naval Hydrophysical Institute. The platform is located near southern coast of Crimea, in the vicinity of Katsiveli village. At this location, the sea depth is approximately 30 m, which for Black Sea corresponds to "deep water" conditions, under which the influence of sea bottom on the wind waves and ripples can be neglected. The minimum distance from the coast was 650 m. The measurements were conducted during summer of 1992. A total of 169 measurement cycles were available for analysis, covering a wide range of hydrometeorological situations.

Statistical characteristics

We choose the coordinate system whose X-axis is oriented along the wind direction and Y-axis oriented across the wind. We introduce the following notations: ξ is the elevation of the sea surface; $\xi_u = d\xi/dx$ and $\xi_c = d\xi/dy$ are the along- and cross-wind components of the surface slopes; $\xi_m = \sqrt{\xi_u^2 + \xi_c^2}$ is the modulus of (or total) slope. From here on, subscripts u and c stand for along- and cross-wind slope components, respectively. The variances of modulus and directional components of the slopes will be denoted, respectively, by σ_m^2, σ_u^2, and σ_c^2; the total variance by $D^2 = \sigma_u^2 + \sigma_c^2$; and the mean modulus of a slope by $\overline{\xi}_m$.

Also, we introduce the notation for parameters characterizing the succession of glares due to specular reflection during the measurement period; they include sampling rate F of glares; mean glare duration τ; and the mean glare intensity I.

To see how relationship between the studied parameters changes in different situations, we used two independent datasets. The first dataset includes measurement data obtained under conditions characteristic of summer season, when water–air stratification is unstable or close to neutral. The sea surface roughness is determined mainly by wind speed and acceleration length of the dominating waves. The measurements were carried out both under winds blowing inland (long acceleration length) and offshore (short acceleration length). The wind speed varied from 0.7 to 14.2 m/s.

The second dataset includes the data obtained during the local upwelling, when sea surface temperature rapidly changed from 21 to 8°C in a few

hours.[11] In this time period, sea roughness is influenced by many physically diverse factors; they include change in momentum flux from wind to waves due to changes in stratification of the near-water atmospheric layer[12]; perturbation of surface flow due to intense dynamic processes in the sea surface layer during upwelling and downwelling motions of cold deep waters[11]; and variations of kinematic viscosity of water due to variations of its temperature.[13] The measurements were carried out under wind speed from 0.7 to 11.9 m/s for both short and long acceleration lengths. These data were obtained under atypical conditions; so they were not analyzed in detail and merely used here to estimate the correlation coefficients.

Table 1 presents correlation matrices, which characterize the relationship between the wind speed, local sea surface characteristics, and the glare statistics. As seen, the estimates for the two data sets agree pretty well. From the fact that wind speed and parameters $\bar{\xi}_m$, σ_m, and D are closely related it follows that the main contribution to these parameters comes from high-frequency components of wave field. As is well known, the spectra of capillary, capillary-gravity, and shortest gravity waves are functions of the wind speed.[14] The larger the wind speed, the greater the sea surface roughness, and, hence, the higher are, e.g., $\bar{\xi}_m$, σ_m, and D.

Table 1. Correlation matrices (30 s averaging time)

Data set I (56 measurement cycles)

	W	$\bar{\xi}_m$	σ_m	D	F	τ	I
W	1	0.81	0.80	0.84	0.72	−0.80	−0.51
$\bar{\xi}_m$	0.81	1	0.98	0.99	0.75	−0.82	−0.50
σ_m	0.80	0.98	1	0.98	0.76	−0.82	−0.53
D	0.84	0.99	0.98	1	0.75	−0.83	−0.51
F	0.72	0.75	0.76	0.75	1	−0.89	−0.84
τ	−0.80	−0.82	−0.82	−0.83	−0.89	1	0.73
I	−0.51	−0.50	−0.53	−0.51	−0.84	0.73	1

Data set II (113 measurement cycles)

	W	$\bar{\xi}_m$	σ_m	D	F	τ	I
W	1	0.85	0.78	0.86	0.95	−0.91	−0.76
$\bar{\xi}_m$	0.85	1	0.97	0.99	0.77	−0.82	−0.85
σ_m	0.78	0.97	1	0.96	0.66	−0.76	−0.85
D	0.86	0.99	0.96	1	0.78	−0.82	−0.82
F	0.95	0.77	0.66	0.78	1	−0.89	−0.66
τ	−0.91	−0.82	−0.76	−0.82	−0.89	1	0.73
I	−0.76	−0.85	−0.85	−0.82	−0.66	0.73	1

The growth of $\bar{\xi}_m$, σ_m, and D causes an associated increase in the local surface curvature, which affects the level of correlation among the parameters that characterize the slopes, as well as the glare statistics. This is because the greater the local surface curvature, the lower the intensity of reflected signal, and, starting from some curvature value, the fewer glares falling within photodetector FOV reach the photodetector sensitivity threshold to be recorded by a signal recorder. As the surface curvature grows further, the number of glares with the intensity below some threshold increases; and at wind speeds exceeding some W_0 value, the dependence of the frequency of recording the glares on the parameters W, $\bar{\xi}_m$, σ_m, and D changes its character, namely: with the growing surface roughness the frequency F decreases.

The W_0 value, at which the frequency of recording glares is maximum, depends on both the parameters of optical device (laser power, photodetector sensitivity, aperture diameter, etc.) and on the distance to the reflecting surface.[15] As is evident from Fig. 1, $W_0 \approx 10$ m/s in our case.

The level of correlation between the studied parameters depends on the averaging time. To show this, we calculated the correlation matrix for 2-min series of successive measurement cycles in form the dataset I (Table 2).

Table 2. Correlation matrix (dataset I, 2-min averaging time, 14 measurement series)

	W	$\bar{\xi}_m$	σ_m	D	F	τ	I
W	1	0.85	0.84	0.89	0.78	−0.84	−0.59
$\bar{\xi}_m$	0.85	1	0.99	0.99	0.80	−0.87	−0.59
σ_m	0.84	0.99	1	0.98	0.82	−0.86	−0.61
D	0.89	0.99	0.98	1	0.80	−0.86	−0.58
F	0.78	0.80	0.82	0.80	1	−0.84	0.86
τ	−0.84	−0.87	−0.86	−0.86	−0.84	1	0.87
I	−0.59	−0.59	−0.61	−0.58	−0.86	0.87	1

Comparing Tables 1 and 2, one can see that, as the averaging time changes by a factor of 4, all estimates of the correlation coefficients markedly increase, except for those between $\bar{\xi}_m$, σ_m, and D which are close to unity even in the case of a 30-s averaging.

From the fact that quite high correlation exists it follows that the statistical models can be used for remote determination of the near-water wind speed and parameters of local slopes from data of laser sensing of the sea surface. Figure 2 shows W and $\bar{\xi}_m$ as functions of glare frequency which, after excluding the cases with $W > W_0$, are well fitted by the linear regression curves given by the following formulas:

$$W = 0.95F + 0.49; \quad (1)$$

$$\bar{\xi}_m = 0.0084F + 0.13. \quad (2)$$

The rms errors for W and $\bar{\xi}_m$ are, respectively, 0.84 m/s and 0.012. Since the correlation between $\bar{\xi}_m$, σ_m, and D is close to unity, we restrict ourselves to analysis of how the glare statistics relates to just one of the parameters characterizing the local slopes, namely, to the mean modulus of the slopes $\bar{\xi}_m$.

As seen, W and $\bar{\xi}_m$ depend nonlinearly on τ (Fig. 3).

So, they were approximated by the regression fits of the following form

$$W = 63.54 \cdot \tau^{-1.548}; \quad (3)$$

$$\bar{\xi}_m = 0.3362 \cdot \tau^{-0.405} \quad (4)$$

with the rms errors of 0.9 m/s and 0.011, respectively; τ in ms.

It is worthy to note here that the regression coefficients as defined by Eqs. (1)–(4) are introduced for estimating W and $\bar{\xi}_m$ under specific instrumental and observation conditions, whose change will call for a new calibration of the instrument.

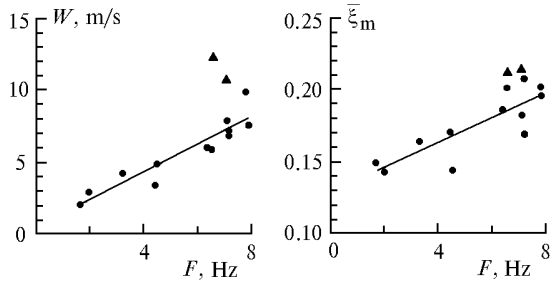

Fig. 2. Wind speed W and mean modulus of the sea surface slope $\bar{\xi}_m$ versus frequency F of recording glares of specular reflection. Triangles show estimates obtained for $W > W_0$. Solid lines show regression curves (1) and (2), respectively.

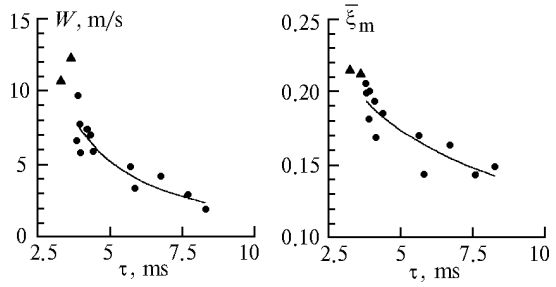

Fig. 3. Wind speed W and mean modulus of the sea surface slope $\bar{\xi}_m$ versus mean duration τ of the glares of specular reflection. Triangles show estimates obtained for $W > W_0$. Solid lines show regression curves (3) and (4), respectively.

Frequency distributions of W and $\bar{\xi}_m$ as functions of I are too complicated. The dependences $W = W(I)$ and $\bar{\xi}_m = \bar{\xi}_m(I)$ in the region of small I values are not single-valued (Fig. 4), which is not yet explained. Possibly, this is due to wave disruption and ensuing surface smoothing, leading to growth of I. However, this issue needs for further study.

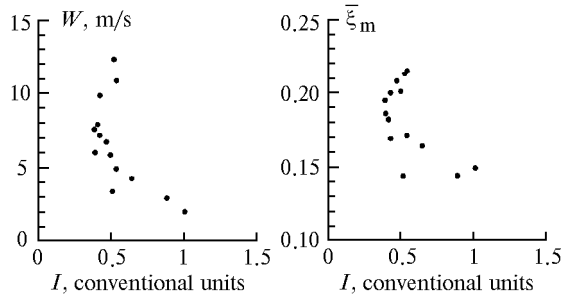

Fig. 4. Wind speed W and mean modulus of the sea surface slope $\bar{\xi}_m$ versus mean intensity I of the glares due to specular reflection.

Conclusions

In this paper we demonstrated that the relationship between statistics of glares due to specular reflection, wind speed, and characteristics of local sea surface slopes has statistical nature. We determined the correlation coefficients for these parameters in two situations, namely, (1) when stratification of near-water atmospheric layer is close to neutral and (2) in the period of local upwelling, and found that they closely agree.

From the fact that the studied parameters are exhibit close correlation it follows that, using laser sensing techniques, it is possible, in principle, to determine the near-water wind speed and characteristics of the local sea surface slopes.

In our experiment, using one-parameter regressions, with the frequency F taken as a parameter, the W and $\bar{\xi}_m$ estimates were obtained with the rms errors of 0.84 m/s and 0.012, respectively (the regressions were plotted using the data obtained under wind speed below 10 m/s). Alternatively, when the mean glare duration τ is used as a parameter, the rms errors for W and $\bar{\xi}_m$ are 0.91 m/s and 0.011, respectively (for $W < 13$ m/s).

Acknowledgments

I would like to conclude by expressing my gratitude to V.E. Smolov and Yu.A. Mishchenchuk for their help in conducting measurements at the oceanographic platform.

References

1. K. Hasselmann, R.K. Raney, W.J. Plant, et al., J. Geophys. Res. **90**, 4659–4686 (1985).
2. A.Yu. Ivanov and K.Ts. Litovchenko, Zarubezhnaya Radioelektronika, No. 2, 18–28 (1999).
3. D.D. Ewans and O.H. Shemdin, J. Geophys. Res. **85**, 5019–5024 (1980).
4. S. Tang and O.H. Shemdin, J. Geophys. Res. **88**, 9832–9840 (1983).
5. M.S. Longe-Higgins, in: *Wind Waves* (Izd. Inostr. Literatury, Moscow, 1962), pp. 125–218.
6. C. Cox and W. Munk, J. Opt. Soc. Am. **44**, No. 11, 838–850 (1954).
7. B.A. Hughes, H.L. Grant, and R.W. Chappell, Deep Sea Res. **24**, No. 12, 1211–1223 (1977).
8. G.N. Khristoforov, A.S. Zapevalov, and M.V. Babii, Okeanologiya **32**, Issue 3, 452–459 (1992).
9. A.P. Aleksandrov and V.P. Legeza, Morsk. Gidrofiz. Zh., No. 6, 51–56 (1988).
10. G. Tober, R.S. Anderson, and O.H. Shemdin, J. Appl. Opt., No. T–4, 788–794 (1973).
11. G.N. Khristoforov and A.S. Zapevalov, Meteorol. Gidrol., No. 7, 64–71 (1997).
12. G.U. Roll, *Physics of Atmospheric Processes over Sea* (Gidrometeoizdat, Leningrad, 1968), 398 pp.
13. R.S. Bortkovskii, Izv. Ros. Akad. Nauk., Ser. Fiz. Atmos. Okeana **33**, No. 2, 266–273 (1997).
14. I.N. Davidan and Yu.A. Trapeznikov, *Gidrometeorologiya*, Ser. Okeanologiya, Issue 1, Obninsk (1981) 46 pp.
15. T.B. Vil'chinskaya and V.G. Mikhalevich, Morsk. Gidrofiz. Zh., No. 6, 57–61 (1990).